Dalton Transactions

COMMUNICATION

View Article Online
View Journal | View Issue

Cite this: *Dalton Trans.*, 2016, **45**, 10519

Received 8th June 2016,
Accepted 10th June 2016

DOI: 10.1039/c6dt02282k

www.rsc.org/dalton

Small, beautiful and magnetically exotic: $\{V_4W_2\}$- and $\{V_4W_4\}$-type polyoxometalates†

Maren Rasmussen,[a] Christian Näther,[a] Jan van Leusen,[b] Ulrike Warzok,[c] Christoph A. Schalley,[c] Paul Kögerler*[b] and Wolfgang Bensch*[a]

Minimal-nuclearity vanadato-tungstate clusters in $[\{V^{IV}(dien)\}_4W^{VI}_2O_{14}]\cdot 4H_2O$ (1) and $[\{V^{IV}(dien)\}_4W^{VI}_4O_{20}]\cdot 6H_2O$ (2) feature cores of edge-sharing WO_6 octahedra, surrounded by a ring of four vanadyl groups. Surprisingly, the V(IV) centers in both 1 and 2 are ferromagnetically coupled, in contrast to all other known vanadato-polyoxotungstates featuring the ubiquituos V–O–W–O–V exchange pathways.

The chemistry of mixed-metal polyoxometalates has witnessed an impressive development during the last few decades, with synthetic and structural aspects, properties and possible applications summarized in several review articles.[1] The first mixed V–W polyanions were reported already in the 19th century;[2] efficient synthesis protocols were developed for the Lindqvist-type polyanions $[V_xW_{6-x}O_{19}]^{-2-x}$ (x = 1, 2),[3] the solution stability of which is strongly pH dependent.[4] The chemistry of mixed tungstato-vanadate compounds was further developed, resulting primarily in several compounds containing $\{V_xW_{6-x}\}$ (x = 1–3) Lindqvist anions, where V and W atoms usually are disordered over all six metal sites.[5] Few other small W/V complexes are known with N- and O-donor ligand environments: in $[L'O(H_2O)V^{IV}(\mu\text{-}O)W^{VI}O_2L]^{2+}$ (L = 1,4,7-triazacyclononane, L′ = 1,4,7-trimethyl-L), VN_3O_2 and WN_3O_2 moieties are μ-oxo-bridged,[6] in $[V_2O_2(\mu\text{-}OMe)_2(\mu\text{-}WO_4)_2(4,4'\text{-di-}tert\text{-butyl-}2,2'\text{-bipyridine})_2]$, two VN_2O_3 units are bridged by two WO_4 groups.[7]

After identifying a $\{V_{13}W_4\}$-type extended Keggin structure under solvothermal conditions at high pH (*ca.* 12) in the presence of tris(2-aminoethyl)amine (tren),[8] we now were able to isolate $[(V(dien))_4W_2O_{14}]\cdot 4H_2O$ (**1**) and $[(V(dien))_4W_4O_{20}]\cdot 6H_2O$ (**2**) (dien = diethylenetriamine, $C_4H_{13}N_3$) under similar conditions, where a higher reactant V : W ratio (1 : 3 *vs.* 1 : 4) appears to favor a smaller W nuclearity.‡ The crystal structures feature rare VN_2O_4 and VN_3O_3 moieties interconnected by edge-sharing WO_6 octahedra (Fig. 1).

Compound **1** crystallizes in the triclinic space group $P\bar{1}$ (Table S1†) with all atoms located on general positions. A W_2O_{10} core composed of two edge-sharing WO_6 octahedra connects to two VON_2 moieties (vanadyl-bidentate diene complexes) *via* three μ-O sites, and edge-sharing to two VON_3 units (vanadyl-tridentate *fac*-dien complexes). The four V sites form a planar rhomboid (V···V: 3.78 Å and 5.38 Å, V–V–V: 70.8°). The N···N distances in the VN_3O_3 octahedron are 2.732, 2.714, and 3.278 Å, and the N–N–N angle amounts to 74°. Vanadium dien complexes are rare, with only two corresponding entries, all of tridentate *fac* conformation, in the CSD.[9] In **1**, V–N bonds in VN_2O_4 and VN_3O_3 (2.116(4)–2.289(4) Å) exhibit a slight elongation of one V–N bond (V1–N2, Fig. S1†), caused by the *trans* effect. The V–O bonds (1.620(3)–2.219(3) Å) show the typical short vanadyl V=O bonds (1.633(4) and 1.620(3) Å). A database analysis (CSD) of compounds containing octahedral VN_2O_4 or VN_3O_3 units yielded a slightly smaller mean value around 1.600 Å. The W–O bonds fall into four groups: 1.752(3) Å (O_{term}), 1.824(3)–1.910(3) Å (μ_2-O), 2.052(3) Å (μ_3-OWV_2), and 2.356(3) Å (μ_3-OW_2V), all typical for polyoxotungstates. In **1**,

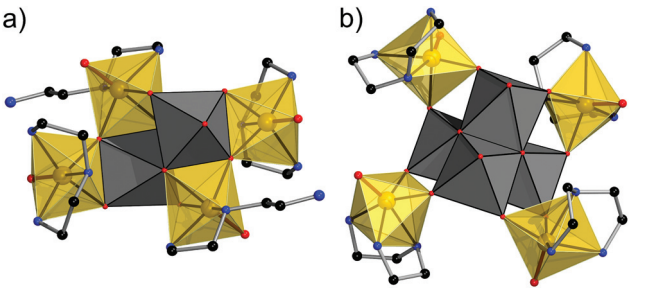

Fig. 1 Combined polyhedral/ball-and-stick plots of the cluster molecules in **1** (a) and **2** (b). WO_6: grey octahedra, O: red, N: blue, C: black, V: yellow spheres. Terminal V=O vanadyl bonds are emphasized in red. H positions omitted for clarity.

[a]*Institut für Anorganische Chemie, Christian-Albrechts-Universität zu Kiel, 24118 Kiel, Germany. E-mail: wbensch@ac.uni-kiel.de*
[b]*Institut für Anorganische Chemie, RWTH Aachen University, 52074 Aachen, Germany. E-mail: paul.koegerler@ac.rwth-aachen.de*
[c]*Institut für Chemie und Biochemie der Freien Universität, 14195 Berlin, Germany*

†Electronic supplementary information (ESI) available: Experimental, crystallographical and structural details, optical properties and thermal stability data. CCDC 1475726 and 1475727. For ESI and crystallographic data in CIF or other electronic format see DOI: 10.1039/c6dt02282k

the [(V(dien))$_4$W$_2$O$_{14}$] complexes are arranged in stacks along [100] and [001], and the inter-cluster voids are occupied by crystal water molecules. Intra-cluster N–H···O and extensive 3D inter-cluster H bonding interactions stabilize the structure. O6$_{term}$ is involved in three relatively strong H bonding contacts, which may explain the longer V=O bond, while O7$_{term}$ has only one such contact (Table S2†). Bond valence sum (BVS) calculations yield values of 4.06/4.09 for V1/V2 and 5.93 for the unique W atom, in line with the formal oxidation states V^{4+} and W^{6+} in **1**.

Compound **2** crystallizes in the monoclinic space group $P2_1/n$ (Table S1†) with all unique atoms being located on general positions. Here, the cluster core consists of four edge-sharing WO_6 octahedra, forming a distorted W_4O_4 cubane. Four independent vanadyl groups each bind to a tridentate dien ligand in *fac* conformation and to two O atoms of neighboring WO_6 octahedra, resulting in distorted VN_3O_3 octahedral environments, with two shorter (2.127(7)–2.175(7) Å) and one longer (2.263(5)–2.318(7) Å) V–N bond, the latter *trans* to the terminal vanadyl O site. The resulting V_4 structure is an approximately planar square (V···V: 5.94–6.22 Å, root mean square deviation from ideal plane: 0.276 Å). The V–O bonds are similar to those in **1** with one short (1.610(6)–1.628(6) Å, V=O$_{term}$) and two longer bonds. The W–O bonds exhibit an identical pattern as in **1**. BVS values (V: 3.97–4.17; W: 5.95–6.09) support the proposed oxidation states.

In **2**, the charge-neutral clusters are arranged in the (010) plane generating channels along [010]. A similar arrangement is observed in the (100) plane, and a second channel type runs along [100]. As in **1**, neighbored clusters are interlinked by N–H···O interactions, in addition to extensive H bonding to the crystal water molecules present in these channels.

The magnetic properties of **1** and **2** are represented in Fig. 2 as χ_mT *vs.* T and M_m *vs.* B plots. For **1**, the ambient temperature (290 K) value of χ_mT is 1.50 cm^3 K mol^{-1} at 0.1 T. This value lies within the range 1.36–1.53 cm^3 K mol^{-1} expected for four non-interacting V^{IV} centers. Upon cooling χ_mT continuously increases up to a maximum of 1.74 cm^3 K mol^{-1} at 14 K, and subsequently drops off sharply down to 0.77 cm^3 K mol^{-1} at 2.0 K. At 2.0 K, the molar magnetization M_m as a function of the applied field B shows an inflection point at *ca.* 2.5 T revealing the presence of minor antiferromagnetic exchange interactions (the inflection point here indicates a change of the total spin ground state). Modeling the magnetic properties of **1** utilized the computational framework CONDON, employing a "full model" Hamiltonian,[10] and assumed four identical V(IV) centers in a C_{4v}-symmetric ligand field, reflecting the pronounced tetragonal distortion typical for vanadyl groups. Five Heisenberg-type exchange interaction pathways between nearest-neighbor V(IV) sites (Fig. 2, inset) are characterized by three independent exchange parameters J_1 (V–O–V and V–O–W^{VI}–O–V), J_2 (V–O–W^{VI}–O–V) and J_3 (2 × V–O–W^{VI}–O–V). The O–W^{VI}–O bridges here efficiently mediate the coupling *via* the extended, unoccupied W 6d orbitals. For fitting purposes, the standard spin–orbit coupling constant ζ_{3d} = 248 cm^{-1} is taken as a constant,[11] and all 10 states of a $3d^1$ electron configuration are accounted for in the calculation of single ion (vanadyl) effects and Heisenberg exchange interactions ("$-2J$" notation), *i.e.* considering in total 10^4 states. Finally, we consider the mean-field approach for potential inter-molecular interactions in the solid-state lattice. The least-squares fit (relative root mean squared error, SQ = 1.7%) yields the ligand field parameters (Wybourne notation) B_0^2 = 4230 cm^{-1}, B_0^4 = 23 250 cm^{-1}, B_4^4 = 31 310 cm^{-1}, the exchange interaction parameters J_1 = +15.6 cm^{-1}, J_2 = −3.7 cm^{-1}, J_3 = +5.9 cm^{-1}, and the mean-field interaction parameter zJ' = +0.1 cm^{-1}. The ligand field parameters B_q^k describe a ligand field characterized by strong tetragonal distortion generating a well-isolated Kramer's ground state doublet separated from the first excited state by more than 4000 cm^{-1}, reconfirming the almost spin-like behavior of the vanadyl groups. The exchange interaction parameters show predominant ferromagnetic exchange, and the additional antiferromagnetic exchange pathways yields a ground state characterized by S_{total} = 0, slightly separated (approx. 2 cm^{-1}) from the first excited S_{total} = 1 state, translating into $M_m \approx 2.0 N_A \mu_B$ as reflected by the inflection point in

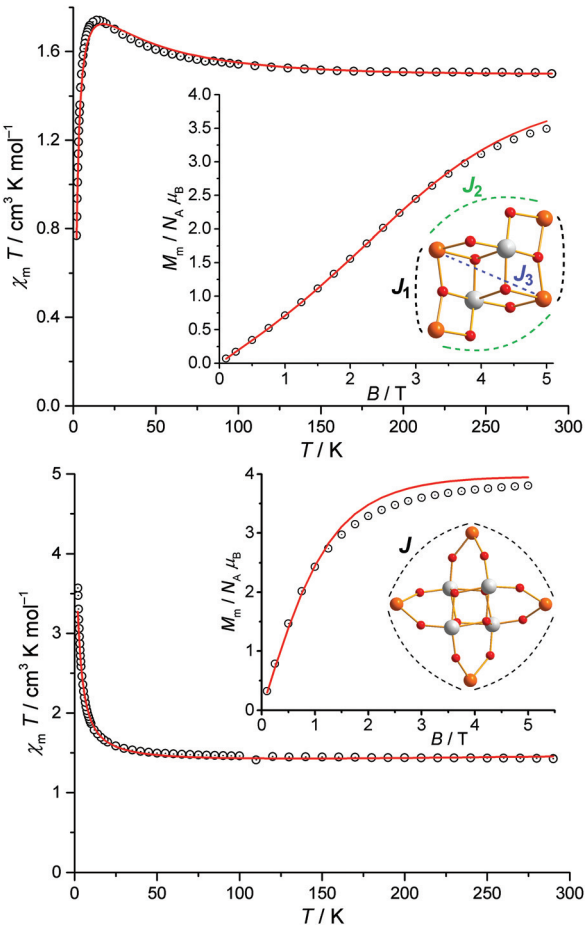

Fig. 2 Magnetic data of compounds **1** (top) and **2** (bottom), and coupling schemes. χ_mT *vs.* temperature T at 0.1 T; insets: molar magnetization M_m *vs.* applied field B at 2.0 K. Open circles: experimental data, red solid lines: least-squares fit.

the M_m *vs.* B curve. Inter-cluster interactions are almost negligible.

The low-field $\chi_m T$ value of **2** at 290 K of 1.45 cm^3 K mol^{-1} falls into the expected range for four non-interacting V^{IV} centers. Upon cooling $\chi_m T$ increases sharply below *ca.* 50 K, reaching 3.57 cm^3 K mol^{-1} at 2.0 K. At 2.0 K, M_m is linear in B up to 1 Tesla, and indicates saturation for fields larger than 5 T at approximately $M_m = 4N_A\mu_B$, *i.e.* pointing to an S_{total} = 2 ground state, *i.e.* in line with dominant ferromagnetic exchange interactions in **2**. In analogy to the analysis of **1** except for the coupling scheme (four V–O–W–O–V pathways characterized by a single exchange energy J), the least-squares fit (SQ = 3.2%) yields B_0^2 = 120 cm^{-1}, B_0^4 = 30 630 cm^{-1}, B_4^4 = 29 460 cm^{-1}, J = +2.7 cm^{-1}, and the mean-field interaction parameter zJ' = +0.1 cm^{-1}. As for **1**, the ligand field parameters here correspond to a strong tetragonal distortion of the V ligand field, generating a well-isolated (*ca.* 6000 cm^{-1}) Kramer's ground state doublet. Note that the common V coordination geometry in **2** is significantly different from **1** (two slightly different site geometries), resulting in different ligand field parameters. The positive J reveals small ferromagnetic nearest-neighbor coupling in **2**. The ground state of **2** amounts to S_{total} = 2, consistent with the observed saturation value of $M_m \approx 4.0N_A\mu_B$. As for **1**, inter-cluster coupling in **2** is almost negligible.

Compound **2** is soluble in water (0.24 mmol L^{-1}), while the solubility of **1** is extremely low. Positive-mode electrospray ionization of a 100 μM water solution of **2** results in an ESI mass spectrum exhibiting the intact cluster as the singly and doubly protonated species at m/z = 836 und 1672 (Fig. 3). The base peak of the spectrum can be assigned to $[(V(dien))_4W_4O_{19}]^{2+}$ which is most likely formed by elimination of H_2O upon protonation of the cluster. Measurements were performed shortly after preparation of the sample solution in degassed H_2O as the cluster complex was only stable in solution over a period of 30 minutes.

In summary, we infer from the two title compounds that the molecular growth of polyoxotungstates at pH *ca.* 12 appears to be impeded by coordination of $VO(dien)^{2+}$ groups and the associated decrease in negative molecular charge, effectively stopping at $\{V_4W_2\}$ and $\{V_4W_4\}$ nuclearities. Comparison to species formed at similar conditions such as the $\{V_{13}W_4\}$-type polyanion emphasizes the crucial role of the employed polyamines. These clusters are among the smallest known heterometal polyoxometalates and as such demonstrate the utility of polydentate ligands such as dien in the isolation of novel polyoxometalates structures. To our great surprise, the resulting exchange pathway geometries allow for ferromagnetic coupling between neighboring vanadyl groups, in stark contrast to the usually strongly antiferromagnetic coupling present in larger vanadato-polyoxometalates featuring similar V^{IV}–O–M^{VI}–O–V^{IV} motifs such as the $\{M_{72}^{VI}V_{30}\}$ Keplerate polyanions.[12]

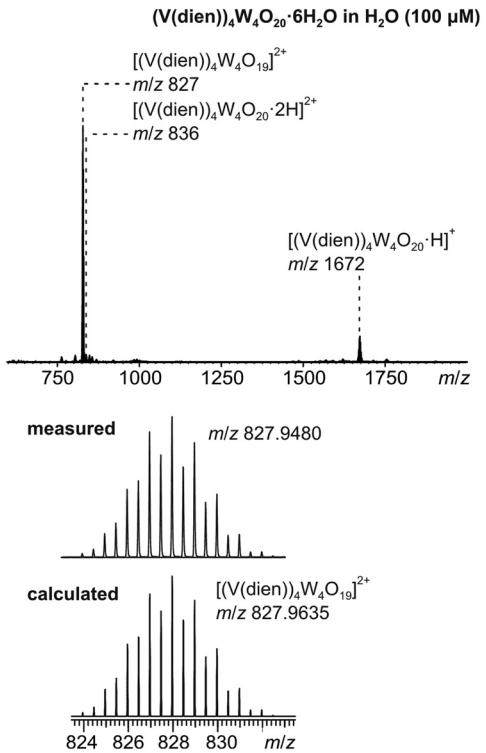

Fig. 3 ESI-Q-TOF-HRMS spectrum of compound **2** (100 μM in H_2O, top); experimental isotopic pattern of dication at m/z 827 and calculated isotopic pattern of $[(V(dien))_4W_4O_{19}]^{2+}$.

Notes and references

‡ Reaction of 1 mmol NH_4VO_3 and 3 mmol $WO_3{\cdot}H_2O$ in a mixture of 2 mL concentrated diethylentriamine and 2 mL water in a sealed glass tube at 130 °C afforded green rod-shaped crystals of **1** after 7 d (70% yield based on V). Orange block-shaped crystals of **2** formed under otherwise identical conditions with 1 mmol NH_4VO_3 and 4 mmol $WO_3{\cdot}H_2O$ (60% yield based on V). CCDC 1475726 (**1**) and 1475727 (**2**).

1 (*a*) O. Oms, A. Dolbecq and P. Mialane, *Chem. Soc. Rev.*, 2012, **41**, 7497; (*b*) K. Y. Monakhov, W. Bensch and P. Kögerler, *Chem. Soc. Rev.*, 2015, **44**, 8443; (*c*) A. Proust, R. Thouvenot and P. Gouzerh, *Chem. Commun.*, 2008, 1837; (*d*) A. Müller, P. Kögerler and H. Bögge, *Struct. Bonding*, 2000, **96**, 203.
2 (*a*) R. Finkener, *Ber. Dtsch. Chem. Ges.*, 1878, **11**, 1638; (*b*) A. Rosenheim and H. Jahn, *Ber. Dtsch. Chem. Ges.*, 1893, **26**, 1191; (*c*) C. Friedheim, *Z. Anorg. Chem.*, 1894, **6**, 11.
3 C. M. Flynn and M. T. Pope, *Inorg. Chem.*, 1971, **10**, 2524.
4 (*a*) C. M. Flynn and M. T. Pope, *Inorg. Chem.*, 1973, **12**, 1626; (*b*) C. M. Flynn and M. T. Pope, *Inorg. Chem.*, 1971, **10**, 2745.
5 (*a*) L. Ouahab, S. Golhen, S. Triki, A. Łapinski, M. Golub and R. Swietlik, *J. Cluster Sci.*, 2002, **13**, 267; (*b*) W. Huang, L. Todaro, L. C. Francesconi and T. Polenova, *J. Am. Chem. Soc.*, 2003, **125**, 5928; (*c*) H. Driss, R. Thouvenot and M. Debbabi, *Polyhedron*, 2008, **27**, 2059; (*d*) J.-H. Son and Y.-U. Kwon, *Inorg. Chem.*, 2004, **43**, 1929; (*e*) P. T. Ma, C. F. Yu, J. W. Zhao, Y. Q. Feng, J. P. Wang and J. Y. Niu, *J. Coord. Chem.*, 2009, **62**, 3117; (*f*) X. Wang, B. Zhou,

C. Zhong and M. Ji, *Cryst. Res. Technol.*, 2006, **41**, 874; (*g*) C. Wang, L. Weng, Y. Ren, C. Du, B. Yue, M. Gu and H. He, *Z. Anorg. Allg. Chem.*, 2011, **637**, 472; (*h*) Y. Xu, J.-Q. Xu, G.-Y. Yang, T.-G. Wang, Y. Xing, Y.-H. Lin and H.-Q. Jia, *Acta Crystallogr., Sect. C: Cryst. Struct. Commun.*, 1998, **54**, 563.

6 U. Bossek, P. Knopp, C. Habenicht, K. Wieghardt, B. Nuber and J. Weiss, *J. Chem. Soc., Dalton Trans.*, 1991, 3165.

7 S. Kodama, A. Nomoto, S. Yano, M. Ueshima and A. Ogawa, *Inorg. Chem.*, 2011, **50**, 9942.

8 M. Rasmussen, C. Näther, J. van Leusen, P. Kögerler and W. Bensch, *Eur. J. Inorg. Chem.*, 2015, 3285.

9 (*a*) M.-L. Fu, G.-C. Guo, A.-Q. Wu, B. Liu, L.-Z. Cai and J.-S. Huang, *Eur. J. Inorg. Chem.*, 2005, 3104; (*b*) J. Wang, C. Näther, J. Djamil and W. Bensch, *Z. Anorg. Allg. Chem.*, 2012, **638**, 1452.

10 (*a*) J. van Leusen, M. Speldrich, H. Schilder and P. Kögerler, *Coord. Chem. Rev.*, 2015, **289–290**, 137; (*b*) M. Speldrich, H. Schilder, H. Lueken and P. Kögerler, *Isr. J. Chem.*, 2011, **51**, 215.

11 J. S. Griffith, *The Theory of Transition-Metal Ions*, Cambridge University Press, Cambridge, 1971.

12 P. Kögerler, B. Tsukerblat and A. Müller, *Dalton Trans.*, 2010, **39**, 21.